Unmanned Systems, Vol. 14, No. 3 (2026) 561–571

DOI: 10.1142/S2301385026410050

Unmanned Systems
https://www.worldscientific.com/worldscinet/us

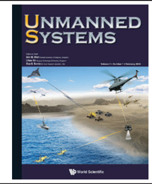

Fixed-Time Time-Varying Group Formation Tracking of Heterogeneous Linear Multi-Agent Systems

Shiyu Zhou [*,‡], Dong Sun [†,§], Gang Feng [*,¶]

[*]*Department of Mechanical Engineering, City University of Hong Kong, Hong Kong, China*

[†]*Department of Biomedical Engineering, City University of Hong Kong, Hong Kong, China*

This paper studies the fixed-time group formation tracking (FXGFT) problem for heterogeneous multi-agent systems (HMASs) under a directed interaction graph. First, a novel distributed fixed-time observer is proposed to estimate the state of each subgroup leader based on both inter-group and intra-group interactions. Then, via a coordinate transformation method, an observer-based fixed-time controller is designed for each follower. It is shown that with the proposed control protocol, the outputs of the followers in each subgroup achieve the desired sub-formation and track the output of the corresponding subgroup leader in a fixed time. Finally, a simulation example demonstrates the effectiveness of the proposed approach.

Keywords: Fixed-time control; formation tracking; group division; multi-agent systems; directed graphs.

1. Introduction

Over the past few decades, the cooperative control of multi-agent systems (MASs) has received considerable attention owing to its wide range of applications, such as unmanned aerial vehicles, autonomous underwater vehicles, and mobile robots [1–8]. Formation control, as a typical class of cooperative control, focuses on coordinating MASs to achieve and maintain specific geometric configurations. Many significant results on the formation control have been reported [9–11]. Formation tracking control of MASs has also been studied [12–17]. In this case, MASs not only form the prescribed formation but also follow the reference trajectory provided by a real or virtual leader.

The existing works on cooperative control primarily concentrate on a single group of agents. However, in some scenarios involving complex and challenging objectives, the group synchronization problem arises, wherein the entire MAS is partitioned into multiple subgroups that perform different tasks simultaneously. Several studies have addressed group synchronization control problems for homogeneous MASs [18–23]. However, due to differences in physical properties or operating conditions, the dynamics of MASs are often nonidentical and therefore are known as HMASs. Compared to homogeneous MASs, HMASs enable better resource utilization, task specialization, and adaptability to complex environments. Recently, several studies have investigated the group cooperative control problem for HMASs [24–26].

The convergence rate serves as a crucial performance index in the study of cooperative control. Most existing research focuses on asymptotic convergence [24–26], where the objective is achieved as time tends to infinity. Due to its advantages, such as faster error convergence and enhanced robustness, finite-time cooperative control of MASs has attracted considerable attention [27–32]. However, a notable drawback of finite-time control is that the upper bound of the convergence time relies on the initial states of the system, which may become excessively large when these states are far from the equilibrium. Motivated by the fixed-time control strategy developed for single systems [33], several studies

Received 10 October 2025; Accepted 10 December 2025; Published 8 January 2026. This paper was recommended for publication in its revised form by Special Issue Editors, Jie Chen, Ben M Chen, and Zongli Lin.
Email Addresses: [‡]*shiyuzhou9-c@my.cityu.edu.hk*; [§]*medsun@cityu.edu.hk*; [¶]*megfeng@cityu.edu.hk*.
[¶]Corresponding author.

have investigated the fixed-time cooperative control problem of MASs [34–39]. Considering both fast error convergence and multi-group cooperation, several finite-time and fixed-time group cooperative control problems have been investigated [40–42]. However, most of these studies focus on integrator-type MASs or homogeneous MASs, and their control protocols are typically designed for undirected interaction graphs. In fact, to our best knowledge, the FXGFT control problem for HMASs under the directed graph is yet to be addressed, which motivates this study.

In this paper, the FXGFT problem for HMASs under a directed graph is studied. A novel fixed-time distributed observer is first designed to estimate the leader's state in each subgroup under the directed graph. FXGFT controllers are further developed for each follower to achieve the desired time-varying formation (TVF) while following the trajectory of their respective leader. The main contributions of this paper are outlined as follows:

(1) A novel distributed FXGFT control protocol, consisting of distributed fixed-time observers and controllers, is developed. Taking into account both inter-group interactions and intra-group interactions, a novel distributed fixed-time observer is developed for each follower to estimate the state of the leader in each subgroup. Subsequently, a FXGFT controller is developed for each follower using coordinate transformation methods. Unlike those group cooperation studies in [24–26] with asymptotic convergence, and [42] with finite-time convergence, this work achieves group formation tracking (GFT) control with an explicit upper bound on the convergence time, which is independent of the initial conditions of the HMAS.
(2) In contrast to the studies in [40–42], which focus on undirected graphs, this paper addresses the FXGFT control problem with more general directed graphs. The asymmetry of the Laplacian matrix in directed graphs complicates both controller design and stability analysis relative to the symmetric case. Moreover, as directed graphs are commonly encountered in practical applications, the proposed FXGFT control protocol is expected to have broader real-world applications.
(3) This paper investigates the FXGFT problem for heterogeneous linear MASs, encompassing integrator-type dynamics discussed in [40, 41] and homogeneous dynamics studied in [42] as special cases.

The remainder of this paper is structured as follows. Section 2 introduces the preliminaries and formulates the FXGFT problem. The main results are presented in Sec. 3. Section 4 provides a numerical simulation, and the conclusions are summarized in Sec. 5.

Notation: Let $\mathbf{1}_n$ and $\mathbf{0}_n$ represent the $n \times 1$ vectors with all entries equal to one and zero, respectively. $\mathrm{I}_n \in \mathbb{R}^{n\times n}$ denotes the identity matrix, and $\otimes$ stands for the Kronecker product. A diagonal matrix is expressed as $\mathrm{diag}\{b_1, \dots, b_n\}$, where b_i, $i = 1, \dots, n$, are its diagonal entries. For a vector $V = [v_1, \dots, v_n]^\top \in \mathbb{R}^n$, its p-norm is represented by $\|V\|p \overset{\Delta}{=} (\sum_{i=1}^n |v_i|^p)^{\frac{1}{p}}$, where $p > 1$. $\|V\|$ represents the Euclidean norm of the vector V. Define $\mathrm{sign}^q(V) = [\mathrm{sign}(v_1)|v_1|^q, \dots, \mathrm{sign}(v_n)|v_n|^q]^\top$, where $q > 0$ and $\mathrm{sign}(\cdot)$ denotes a sign function. The operators $\min(\cdot)$ and $\max(\cdot)$ return the smallest and largest elements of a vector, respectively.

2. Preliminaries and Problem Formulation

2.1. *Graph theory*

The directed interaction graph among the MASs is represented by $\mathcal{G} = (\mathcal{O}, \mathcal{E}, \mathcal{A})$ with the set of nodes $\mathcal{O} = \{1, \dots, N\}$, the set of edges $\mathcal{E} = \{(j, i) : i, j \in \mathcal{O}\}$, and the weighted adjacency matrix $\mathcal{A} = [a_{ij}] \in \mathbb{R}^{N\times N}$, where $a_{ij} \neq 0$ if $(j, i) \in \mathcal{E}$, and $a_{ij} = 0$ otherwise.

Consider a HMAS with N_f followers and N_l leaders. If an agent has no neighbors, it is defined as a leader; otherwise, it is defined as a follower. Let $\mathcal{O}_l = \{1, \dots, N_l\}$ and $\mathcal{O}_f = \{1, \dots, N_f\}$ be the sets of the followers and leaders, respectively. The set of followers $\mathcal{O}_f$ is partitioned into $\{\mathcal{O}_{f1}, \mathcal{O}_{f2}, \dots, \mathcal{O}_{fN_l}\}$ such that $\mathcal{O}_{fj} \neq \emptyset$, $\bigcup_{j=1}^{N_l} \mathcal{O}_{fj} = \mathcal{O}_f$, and $\mathcal{O}_{fj} \cap \mathcal{O}_{fs} = \emptyset$ for $j, s = 1, \dots, N_l$, $j \neq s$. The system is divided into N_l subgroups, represented by $\mathcal{O}_r$, $r = 1, \dots, N_l$, where each subgroup $\mathcal{O}_r$ contains the rth leader together with its corresponding follower subset $\mathcal{O}_{fr}$. The number of the followers associated with subgroup r is denoted by g_r satisfying $\sum_{r=1}^{N_l} g_r = N_f$.

2.2. *Problem formulation*

The model of the ith follower is described by

$$\begin{aligned} \dot{x}_i(t) &= A_i x_i(t) + B_i u_i(t), \\ y_i(t) &= C_i x_i(t), \end{aligned} \tag{1}$$

where $x_i \in \mathbb{R}^{n_i}$, $u_i \in \mathbb{R}^{m_i}$, $y_i \in \mathbb{R}^p$ represent the state, control input, and output of the ith follower, respectively, A_i, B_i, and C_i are the system matrices of compatible dimensions satisfying $\mathrm{rank}(B_i) = m_i$.

The leader indexed by $0r$ for subgroup $\mathcal{O}_r$ evolves according to the following dynamics:

$$\begin{aligned} \dot{x}_{0r}(t) &= A_0 x_{0r}(t), \\ y_{0r}(t) &= C_0 x_{0r}(t), \end{aligned} \tag{2}$$

where $x_{0r} \in \mathbb{R}^{n_0}$, and $y_{0r} \in \mathbb{R}^p$ are the state and output of the rth leader, respectively, A_0 and C_0 are matrices of compatible dimensions.

The TVF vector for the ith follower is generated by

$$\begin{aligned}\dot{h}_{xi}(t) &= A_F h_{xi}(t),\\ h_{yi}(t) &= C_F h_{xi}(t),\end{aligned} \tag{3}$$

where $h_{yi} \in \mathbb{R}^p$, A_F and C_F are matrices of compatible dimensions.

The objective of this paper is to address the following problem.

Definition 2.1 (FXGFT problem). Consider the HMAS (1) and (2) under a directed graph. For each follower in any subgroup $\mathcal{O}_r = \{\text{leader } r, \mathcal{O}_{fr}\}$, $r = 1, \dots, N_l$, the FXGFT problem is defined to be finding a distributed fixed-time control protocol such that

$$\lim_{t\to T} \|y_i(t) - h_{yi}(t) - y_{0r}(t)\| = 0, \quad \forall i \in \mathcal{O}_{fr}, \tag{4}$$

where $T > 0$ represents the convergence time that is independent of the initial states.

Remark 1. According to Definition 2.1, the outputs of the followers in each subgroup are required to achieve the TVF and track the output of their subgroup leader in a fixed time. For follower i in subgroup $\mathcal{O}_r$, the TVF vector h_{yi}, which is generated by Eq. (3), represents the desired relative offset between the output y_i and the reference output y_{0r}.

To address the problem, the following assumptions and lemmas are presented.

Assumption 1. The pair (A_i, B_i) is controllable, $i \in \mathcal{O}_f$.

Assumption 2. The following regulator equations:

$$\begin{aligned}\Pi_i A_0 &= A_i \Pi_i + B_i \Gamma_i,\\ 0 &= C_i \Pi_i - C_0\end{aligned} \tag{5}$$

have solution pairs (Π_i, Γ_i) for all $i \in \mathcal{O}_f$.

Assumption 3. The following linear matrix equations:

$$\begin{aligned}\Pi_{Fi} A_F &= A_i \Pi_{Fi} + B_i \Gamma_{Fi},\\ 0 &= C_i \Pi_{Fi} - C_F\end{aligned} \tag{6}$$

have solution pairs (Π_{Fi}, Γ_{Fi}) for all $i \in \mathcal{O}_f$.

Assumption 4. The partition of followers $\mathcal{O}_f$ given by $\{\mathcal{O}_{f1}, \dots, \mathcal{O}_{fN_l}\}$ is acyclic.

The Laplacian matrix among the agents has the following form:

$$\mathcal{L} = \begin{bmatrix} \mathcal{L}_1 & \mathcal{L}_2 \\ \mathbf{0}_{N_l\times N_f} & \mathbf{0}_{N_l\times N_l}\end{bmatrix},$$

where $\mathcal{L}_1 \in \mathbb{R}^{N_f\times N_f}$ and $\mathcal{L}_2 \in \mathbb{R}^{N_f\times N_l}$. As described in [19], under Assumption 4, $\mathcal{L}_1$ has the following particular structure:

$$\mathcal{L}_1 = \begin{bmatrix} \bar{\mathcal{L}}_1 & \mathbf{0}_{g_1\times g_2} & \cdots & \mathbf{0}_{g_1\times g_{N_l}} \\ \bar{\mathcal{L}}_{21} & \ddots & & \mathbf{0}_{g_2\times g_{N_l}} \\ \vdots & \bar{\mathcal{L}}_{ij} & \ddots & \vdots \\ \bar{\mathcal{L}}_{N_l 1} & \cdots & \cdots & \bar{\mathcal{L}}_{N_l}\end{bmatrix},$$

where $\bar{\mathcal{L}}_i$ denotes the interaction graph within subgroup $\mathcal{O}_i$. $\bar{\mathcal{L}}_{ij}$ represents the interaction graph between the followers of subgroups $\mathcal{O}_i$ and $\mathcal{O}_j$, $i \neq j$.

Assumption 5. Given any two different subgroups $\mathcal{O}_i$ and $\mathcal{O}_j$, $i, j \in \{1, \dots, N_l\}$, the row sums of $\bar{\mathcal{L}}_{ij}$ are all zero.

Assumption 6. The interaction graph of any subgroup $\mathcal{O}_k = \{\text{leader } k, \mathcal{O}_{fk}\}$, $k = 1, \dots, N_l$, contains a spanning tree with leader k as the root.

Remark 2. Assumptions 1–3 are standard for the cooperative control problem of HMASs [15,28,35]. According to [43], the regulator Eq. (5) admits solutions if $\operatorname{rank}\begin{bmatrix} A_i - \lambda \mathrm{I}_{n_i} & B_i \\ C_i & 0\end{bmatrix} = n_i + p$ holds for all $\lambda \in \sigma(A_0)$, where $\sigma(A_0)$ denotes the spectrum of A_0. Assumptions 4–6 are commonly made in group synchronization problems [22–26].

Lemma 1 ([22]). *Under Assumptions* 4–6, *all eigenvalues of $\mathcal{L}_1$ have positive real parts, and $-\mathcal{L}_1^{-1}\mathcal{L}_2$ has the following form*:

$$-\mathcal{L}_1^{-1}\mathcal{L}_2 = \begin{bmatrix} \mathbf{1}_{g_1} & \mathbf{0}_{g_1} & \cdots & \mathbf{0}_{g_1} \\ \mathbf{0}_{g_2} & \mathbf{1}_{g_2} & \cdots & \mathbf{0}_{g_2} \\ \vdots & \vdots & \ddots & \vdots \\ \mathbf{0}_{g_{N_l}} & \mathbf{0}_{g_{N_l}} & \cdots & \mathbf{1}_{g_{N_l}}\end{bmatrix}.$$

Lemma 2 ([23]). *Under Assumptions* 4–6, *one can find a real diagonal matrix $\bar{\mathcal{D}}$ satisfying $\bar{\mathcal{D}}\mathcal{L}_1 + \mathcal{L}_1^{\top}\bar{\mathcal{D}} > 0$.*

Define $\lambda_{\min} > 0$ as the minimal eigenvalue of $\bar{\mathcal{D}}\mathcal{L}_1 + \mathcal{L}_1^{\top}\bar{\mathcal{D}}$ and $\mathcal{D} = \operatorname{diag}\{d_1, \dots, d_{N_f}\} = \frac{2\bar{\mathcal{D}}}{\lambda_{\min}}$, where $d_i > 0$, $i = 1, \dots, N_f$. By Lemma 2, it follows that $\mathcal{D}\mathcal{L}_1 + \mathcal{L}_1^{\top}\mathcal{D} \geq 2\mathrm{I}_{N_f}$.

3. Main Results

This section presents a novel distributed fixed-time observer under the directed interaction graph. Then, an observer-based FXGFT controller is designed.

3.1. *Distributed fixed-time observers*

For each follower in any subgroup $\mathcal{O}_r = \{\text{leader } r, \mathcal{O}_{fr}\}$, $r = 1, \dots, N_l$, the following distributed fixed-time observer is proposed:

$$\dot{v}_i = A_0 v_i - k_1\delta_i - k_2\,\mathrm{sign}^p(\delta_i) - k_3\,\mathrm{sign}^q(\delta_i), \tag{7a}$$

$$\delta_i = \sum_{j=1}^{N_f} a_{ij}(v_i - v_j) + \sum_{k=1}^{N_l} a_{i0k}(v_i - x_{0k}), \tag{7b}$$

where v_i represents the state of the observer, δ_i denotes the neighboring relative estimation error, and the parameters k_1, k_2, k_3, p, and q are positive constants that will be decided later.

Define the estimation error $\tilde{v}_i = v_i - x_{0r}$. Then, the following result on the distributed observer (7) is given.

Theorem 1. *Consider the distributed observers* (7) *under Assumptions* 4–6*. Let k_1, k_2, k_3, p, and q be chosen such that $k_1 > \|\mathcal{D}\otimes A_0\|$, $k_2 > 0$, $k_3 > 0$, $0 < p < 1$, and $q > \frac{1}{p} > 1$. For each follower in any subgroup $\mathcal{O}_r = \{\text{leader } r, \mathcal{O}_{fr}\}$, $r = 1,\dots,N_l$, there is a convergence time $T_1 \geq 0$, independent of any initial conditions, such that $\lim_{t\to T_1}\tilde{v}_i(t) = 0$ and $\tilde{v}_i(t) = 0$, $t \geq T_1$.*

Proof. It then follows from (2) and (7) that

$$\dot{\tilde{v}}_i = A_0\tilde{v}_i - \bar{\delta}_i, \tag{8}$$

where $\bar{\delta}_i = k_1\delta_i + k_2\,\mathrm{sign}^p(\delta_i) + k_3\,\mathrm{sign}^q(\delta_i)$.

Let $\tilde{v} = [\tilde{v}_1^\top,\dots,\tilde{v}_{N_f}^\top]^\top$ and $\bar{\delta} = [\bar{\delta}_1^\top,\dots,\bar{\delta}_{N_f}^\top]^\top$. One can obtain from (8) that

$$\dot{\tilde{v}} = (\mathrm{I}_{N_f}\otimes A_0)\tilde{v} - \bar{\delta}. \tag{9}$$

Let $v = [v_1^\top,\dots,v_{N_f}^\top]^\top$, $x_0 = [x_{01}^\top,\dots,x_{0N_l}^\top]^\top$, and $\delta = [\delta_1^\top,\dots,\delta_{N_f}^\top]^\top$. It follows from Lemma 1 that $\tilde{v} = v + ((\mathcal{L}_1^{-1}\mathcal{L}_2)\otimes \mathrm{I}_{n_0})x_0$ and $\delta = (\mathcal{L}_1\otimes\mathrm{I}_{n_0})v + (\mathcal{L}_2\otimes\mathrm{I}_{n_0})x_0 = (\mathcal{L}_1\otimes\mathrm{I}_{n_0})\tilde{v}$. Then, by (9), one has

$$\dot{\delta} = (\mathrm{I}_{N_f}\otimes A_0)\delta - (\mathcal{L}_1\otimes\mathrm{I}_{n_0})\bar{\delta}. \tag{10}$$

Choose the following Lyapunov function candidate:

$$V_\delta = \sum_{i=1}^{N_f}\left(\frac{k_2 d_i}{1+p}\|\delta_i\|_{1+p}^{1+p} + \frac{k_3 d_i}{1+q}\|\delta_i\|_{1+q}^{1+q}\right) + \frac{k_1}{2}\delta^\top(\mathcal{D}\otimes\mathrm{I}_{n_0})\delta. \tag{11}$$

The time derivative of (11) along (10) satisfies

$$\begin{aligned}\dot{V}_\delta &= \sum_{i=1}^{N_f}(k_2 d_i\,\mathrm{sign}^p(\delta_i) + k_3 d_i\,\mathrm{sign}^q(\delta_i))^\top\dot{\delta}_i + k_1\delta^\top(\mathcal{D}\otimes\mathrm{I}_{n_0})\dot{\delta}\\ &= \bar{\delta}^\top(\mathcal{D}\otimes A_0)\delta - \frac{1}{2}\bar{\delta}^\top((\mathcal{D}\mathcal{L}_1 + \mathcal{L}_1^\top\mathcal{D})\otimes\mathrm{I}_{n_0})\bar{\delta}.\end{aligned} \tag{12}$$

Noting that $\mathcal{D}\mathcal{L}_1 + \mathcal{L}_1^\top\mathcal{D} \geq 2\mathrm{I}_{N_f}$, via Young's inequality, one can obtain from (12) that

$$\dot{V}_\delta \leq \frac{1}{2}(\|\mathcal{D}\otimes A_0\|^2\|\delta\|^2 - \|\bar{\delta}\|^2). \tag{13}$$

Since $k_1\delta_i$, $k_2\,\mathrm{sign}^p(\delta_i)$, and $k_3\,\mathrm{sign}^q(\delta_i)$ are of component-wise sign consistency with their respective elements, one has

$$\begin{aligned}\|\bar{\delta}\|^2 &= \sum_{i=1}^{N_f}\|k_1\delta_i + k_2\,\mathrm{sign}^p(\delta_i) + k_3\,\mathrm{sign}^q(\delta_i)\|^2\\ &\geq \sum_{i=1}^{N_f}k_1^2\|\delta_i\|^2 + \sum_{i=1}^{N_f}k_2^2\|\delta_i\|_{2p}^{2p} + \sum_{i=1}^{N_f}k_3^2\|\delta_i\|_{2q}^{2q}.\end{aligned} \tag{14}$$

Noting that $0 < p < 1$ and $q > 1$, by Lemma A.1 given in Appendix A, one has $\sum_{i=1}^{N_f}\|\delta_i\|_{2p}^{2p} \geq (\|\delta\|^2)^p$ and $\sum_{i=1}^{N_f}\|\delta_i\|_{2q}^{2q} \geq \frac{1}{(n_0N_f)^{q-1}}(\|\delta\|^2)^q$. Then, it follows from (14) that

$$\|\bar{\delta}\|^2 \geq k_1^2\|\delta\|^2 + k_2^2(\|\delta\|^2)^p + \frac{k_3^2}{(n_0N_f)^{q-1}}(\|\delta\|^2)^q. \tag{15}$$

Substituting (15) into (13), one has

$$\dot{V}_\delta \leq -c_1(\|\delta\|^2 + (\|\delta\|^2)^p + (\|\delta\|^2)^q), \tag{16}$$

where $c_1 = \min\{\frac{k_1^2 - \|\mathcal{D}\otimes A_0\|^2}{2}, \frac{k_2^2}{2}, \frac{k_3^2}{2(n_0N_f)^{q-1}}\} > 0$.

Since $0 < p < 1$ and $q > 1$, via Lemma A.1, one has $\sum_{i=1}^{N_f}\frac{k_2 d_i}{1+p}\|\delta_i\|_{1+p}^{1+p} \leq \bar{k}_2(\|\delta\|^2)^{\frac{1+p}{2}}$ and $\sum_{i=1}^{N_f}\frac{k_3 d_i}{1+q}\|\delta_i\|_{1+q}^{1+q} \leq \bar{k}_3(\|\delta\|^2)^{\frac{1+q}{2}}$, where $\bar{k}_2 = (\frac{k_2 d_{\max}}{1+p})(n_0N_f)^{\frac{1-p}{2}}$, $\bar{k}_3 = \frac{k_3 d_{\max}}{1+q}$, and $d_{\max} = \max\{d_1,\dots,d_{N_f}\}$. Note that $0 < \frac{2p}{1+p} < 1$ and $\frac{2q}{1+q} > 1$. Via (11) and Lemma A.1, one has

$$V_\delta^{\frac{2p}{1+p}} \leq c_2\big((\|\delta\|^2)^{\frac{2p}{1+p}} + (\|\delta\|^2)^p + (\|\delta\|^2)^{\frac{p(1+q)}{1+p}}\big) \tag{17}$$

and

$$V_\delta^{\frac{2q}{1+q}} \leq c_3\big((\|\delta\|^2)^{\frac{2q}{1+q}} + (\|\delta\|^2)^{\frac{q(1+p)}{1+q}} + (\|\delta\|^2)^q\big), \tag{18}$$

where $c_2 = \max\{(\frac{k_1 d_{\max}}{2})^{\frac{2p}{1+p}}, \bar{k}_2^{\frac{2p}{1+p}}, \bar{k}_3^{\frac{2p}{1+p}}\}$ and $c_3 = \max\{(\frac{k_1 d_{\max}}{2})^{\frac{2q}{1+q}}, \bar{k}_2^{\frac{2q}{1+q}}, \bar{k}_3^{\frac{2q}{1+q}}\}\times 3^{\frac{q-1}{q+1}}$.

Since $p < \frac{2p}{1+p} < 1$ and $p < \frac{p(1+q)}{1+p} < q$, one has $(\|\delta\|^2)^{\frac{2p}{1+p}} \leq \|\delta\|^2 + (\|\delta\|^2)^p$ and $(\|\delta\|^2)^{\frac{p(1+q)}{1+p}} \leq (\|\delta\|^2)^p + (\|\delta\|^2)^q$. Similarly, noting that $1 < \frac{2q}{1+q} < q$ and $q < \frac{q(1+p)}{1+q} <$

q, one has $(\|\delta\|^2)^{\frac{2q}{1+q}} \le \|\delta\|^2 + (\|\delta\|^2)^q$ and $(\|\delta\|^2)^{\frac{q(1+p)}{1+q}} \le (\|\delta\|^2)^p + (\|\delta\|^2)^q$. Then, via (17) and (18), one has

$$V_\delta^{\frac{2p}{1+p}} \le c_2\big(\|\delta\|^2 + 3(\|\delta\|^2)^p + (\|\delta\|^2)^q\big) \tag{19}$$

and

$$V_\delta^{\frac{2q}{1+q}} \le c_3\big(\|\delta\|^2 + 3(\|\delta\|^2)^q + (\|\delta\|^2)^p\big). \tag{20}$$

Combining (19) and (20), one has

$$\frac{V_\delta^{\frac{2p}{1+p}}}{4c_2} + \frac{V_\delta^{\frac{2q}{1+q}}}{4c_3} \le \|\delta\|^2 + (\|\delta\|^2)^q + (\|\delta\|^2)^p. \tag{21}$$

Substituting (21) into (16), one has

$$\dot V_\delta \le -\frac{c_1}{4c_2} V_\delta^{\frac{2p}{1+p}} - \frac{c_1}{4c_3} V_\delta^{\frac{2q}{1+q}}. \tag{22}$$

By Lemma A.2 in Appendix A, it follows that system (10) is fixed-time stable. The convergence time can be upper bounded by $T_1 \le \frac{4c_2(1+p)}{c_1(1-p)} + \frac{4c_3(1+q)}{c_1(q-1)}$. Moreover, since $\delta(t) = (\mathcal{L}_1 \otimes \mathrm{I}_{n_0})\tilde v(t)$ and $\mathcal{L}_1$ is nonsingular, one has $\lim_{t\to T_1} \tilde v_i(t) = 0$ and $\tilde v_i(t) = 0$ for $t \ge T_1$. Thus, the proof is completed. □

3.2. *FXGFT controller*

Based on the distributed fixed-time observers described in (7), we proceed to develop the FXGFT controller in this part.

The following observer-based FXGFT controller is proposed.

$$u_i(t) = \Gamma_i v_i(t) + \Gamma_{Fi} h_{xi}(t) + \mu_i(t), \quad i \in \mathcal{O}_f, \tag{23}$$

where Γ_i and Γ_{Fi} are the solutions to Eqs. (4) and (5), respectively, $\mu_i(t)$ will be determined later.

Let $\hat e_i = x_i - \Pi_i v_i - \Pi_{Fi} h_{xi}$. Noting that $\mathrm{rank}(B_i) = m_i$, via Assumption 1 and Lemma A.3 given in Appendix A, one can find a linear coordinate transformation $\hat\varepsilon_i = X_i \hat e_i = [\hat\varepsilon_{i1,1}, \dots, \hat\varepsilon_{i1,\rho_1}, \dots, \hat\varepsilon_{im_i,1}, \dots, \hat\varepsilon_{im_i,\rho_{m_i}}]^\top$, where ρ_j, $j = 1, \dots, m_i$, denotes the controllability index of $\hat\varepsilon_{ij}$.

Then, $\mu_i(t)$ can be designed as follows:

$$\mu_i = M_i^{-1}(\omega_i - G_i \hat\varepsilon_i), \tag{24}$$

where $\omega_i = [\omega_{i1}, \dots, \omega_{ij}, \dots, \omega_{im_i}]^\top$ with $\omega_{ij} = -\sum_{k=1}^{\rho_j} \times (c_{ij,k}\,\mathrm{sign}^{r_{ij,k}}(\hat\varepsilon_{ij,k}) + \bar c_{ij,k}\,\mathrm{sign}^{l_{ij,k}}(\hat\varepsilon_{ij,k}))$, G_i and M_i are given as in Lemma A.3, $c_{ij,k}$, $\bar c_{ij,k}$, $r_{ij,k}$, and $l_{ij,k}$, $j = 1, \dots, m_i$, $k = 1, \dots, \rho_j$ can be determined according to Lemma A.4 in Appendix A.

Now, the main result of this work is presented as follows.

Theorem 2. *Suppose Assumptions* 1–6 *hold. Consider the HMAS* (1) *and* (2)*. The distributed FXGFT problem is solved by the distributed control protocols consisting of* (7), (23), *and* (24)*.*

Proof. The proof is to be accomplished via two steps. First, it is shown that the tracking errors are bounded in $[0, T_1)$. Second, we show that the tracking errors converge to zero in a fixed time.

Step 1: $\hat e_i$ is bounded in $t \in [0, T_1)$.

Under Assumptions 2 and 3, one can obtain from (1), (3), (7), and (23) that

$$\dot{\hat e}_i = A_i \hat e_i + B_i v_i + \Pi_i \bar\delta_i. \tag{25}$$

Let $\hat\varepsilon_i = X_i \hat e_i = [\hat\varepsilon_{i1,1}, \dots, \hat\varepsilon_{i1,\rho_1}, \dots, \hat\varepsilon_{im_i,1}, \dots, \hat\varepsilon_{im_i,\rho_{m_i}}]^\top$ and $\bar\Delta_i = X_i \Pi_i \bar\delta_i = [\bar\Delta_{i1,1}, \dots, \bar\Delta_{i1,\rho_1}, \dots, \bar\Delta_{im_i,1}, \dots, \bar\Delta_{im_i,\rho_{m_i}}]^\top$. Then, the dynamics of $\hat\varepsilon_{ij}$, $j = 1, \dots, m_i$, has the following form:

$$\begin{cases} \dot{\hat\varepsilon}_{ij,1} = \hat\varepsilon_{ij,2} + \bar\Delta_{ij,1}, \\ \dot{\hat\varepsilon}_{ij,2} = \hat\varepsilon_{ij,3} + \bar\Delta_{ij,2}, \\ \quad\vdots \\ \dot{\hat\varepsilon}_{ij,\rho_j} = \displaystyle\sum_{k=1}^{\rho_j} (c_{ij,k}\,\mathrm{sign}^{r_{ij,k}}(\hat\varepsilon_{ij,k}) \\ \qquad\qquad + \bar c_{ij,k}\,\mathrm{sign}^{l_{ij,k}}(\hat\varepsilon_{ij,k})) + \bar\Delta_{ij,\rho_j}. \end{cases} \tag{26}$$

As established in [44], system (26) is bounded-input-bounded-state stable with $\bar\Delta_{ij} = [\bar\Delta_{ij,1}, \dots, \bar\Delta_{ij,\rho_j}]^\top$ regarded as the input. According to Theorem 1, $\bar\delta_i$ is bounded in $[0, T_1)$, and consequently $\bar\Delta_{ij}$, $j = 1, \dots, m_i$, are bounded on the same interval. As a result, $\hat\varepsilon_i$ remains bounded as well. Since $\hat\varepsilon_i = X_i \hat e_i$ and X_i is nonsingular, $\hat e_i$ is also bounded in $[0, T_1)$.

Step 2: Fixed-time convergence of $\hat e_i$.

For $t \ge T_1$, we have $\bar\delta_i = 0$, which yields $\hat e_i = e_i \triangleq x_i - \Pi_i x_{0r} - \Pi_{Fi} h_{xi}$. Noting that $\varepsilon_i = X_i e_i = [\varepsilon_{i1,1}, \dots, \varepsilon_{i1,\rho_1}, \dots, \varepsilon_{im_i,1}, \dots, \varepsilon_{im_i,\rho_{m_i}}]^\top$, the dynamics of ε_{ij}, $j = 1, \dots, m_i$, has the following form:

$$\begin{cases} \dot\varepsilon_{ij,1} = \varepsilon_{ij,2}, \\ \dot\varepsilon_{ij,2} = \varepsilon_{ij,3}, \\ \quad\vdots \\ \dot\varepsilon_{ij,\rho_j} = \displaystyle\sum_{k=1}^{\rho_j} (c_{ij,k}\,\mathrm{sign}^{r_{ij,k}}(\varepsilon_{ij,k}) + \bar c_{ij,k}\,\mathrm{sign}^{l_{ij,k}}(\varepsilon_{ij,k})). \end{cases} \tag{27}$$

By Lemma A.4, it can be concluded that $\forall j \in \{1, \dots, m_i\}$, the system described by (27) is fixed-time stable with convergence time bounded by $T \le T_1 + T_2$, where T_2 is given by Lemma A.4. Since $\varepsilon_i(t) = X_i e_i(t)$, with X_i being invertible, and $e_{yi}(t) = C_i e_i(t) = y_i(t) - h_{yi}(t) - y_{0r}(t)$, one can conclude that $\lim_{t\to T} e_{yi}(t) = 0$ and $e_{yi}(t) = 0$ for $t \geq T$. The proof is thus completed. □

Remark 3. Under Assumption 1 and the condition $\text{rank}(B_i) = m_i$, it follows from Lemma A.3 that there exists a nonsingular matrix M_i for each follower to construct the fixed-time tracking component $\mu_i(t)$.

Remark 4. Compared with existing finite-time results in [27–32], the upper bound of the convergence time in this work is independent of the initial states of the concerned system. Nevertheless, the proposed fixed-time control scheme may require larger control inputs than the aforementioned finite-time approaches, which may pose challenges in energy-limited applications.

Remark 5. By applying a coordinate transformation, system (25) is reformulated as m_i single-input subsystems in the controllable canonical form, where the coupling appears only in the last equation of each block. A fixed-time control scheme is then designed based on Lemma A.4. This design avoids the computation of the generalized inverse of the followers' input matrix and relaxes the common full-row rank assumption adopted in [38, 39].

4. Simulation

This section presents a simulation to demonstrate the effectiveness of the proposed FXGFT control protocol.

The HMAS is partitioned into three subgroups, each with a single leader. Subgroups 1 and 2 each consist of one leader and three followers, whereas subgroup 3 consists of one leader and four followers. In this setting, $\mathcal{O}_{f1} = \{1, 2, 3\}$, $\mathcal{O}_{f2} = \{4, 5, 6\}$, and $\mathcal{O}_{f3} = \{7, 8, 9, 10\}$. The interaction graph is shown in Fig. 1.

As in [15], the system matrices of the followers are described by

$$A_i = \mathrm{I}_2 \otimes \begin{pmatrix} 0 & 1 \\ a_i & b_i \end{pmatrix}, \quad B_i = \mathrm{I}_2 \otimes \begin{pmatrix} 0 \\ 1 \end{pmatrix}, \quad C_i = \mathrm{I}_2 \otimes (1\ 0),$$

$$A_j = \mathrm{I}_2 \otimes 0, \quad B_j = \mathrm{I}_2, \quad C_j = \mathrm{I}_2,$$

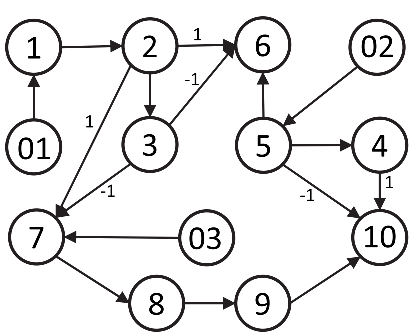

Fig. 1. The interaction graph.

where $i = \{1, \ldots, 8\}$, $j = \{9, 10\}$, the parameters $\{a_i, b_i\}$ are set as $\{-3, -5\}$, $\{-2, -3\}$, $\{-4, -6\}$, $\{-4, -4\}$, $\{-2, -2\}$, $\{-3, -1\}$, $\{-5, -3\}$, and $\{-6, -6\}$, respectively. The reference trajectories are generated in the form of (2) with $A_0 = \mathrm{I}_2 \otimes \begin{pmatrix} 0 & 1 \\ 0 & 0 \end{pmatrix}$ and $C_0 = \mathrm{I}_2 \otimes (1\ 0)$.

The TVF vectors are given as

$$h_{xi}(t) = R_i \begin{pmatrix} \sin(t + \phi_i) \\ \cos(t + \phi_i) \\ \cos(t + \phi_i) \\ -\sin(t + \phi_i) \end{pmatrix}, \quad i = 1, \ldots, 10,$$

where

$$\phi_i = \begin{cases} \dfrac{(i-1)2\pi}{3}, & i \in \mathcal{O}_{f1}, \\ \dfrac{(i-4)2\pi}{3}, & i \in \mathcal{O}_{f2}, \\ \dfrac{(i-7)\pi}{2}, & i \in \mathcal{O}_{f3}, \end{cases}$$

$R_i = 12$, and $C_F = \mathrm{I}_2 \otimes \begin{pmatrix} 1 & 0 \end{pmatrix}$. Solving the linear matrix Eqs. (5) and (6) yields $\Pi_i = \mathrm{I}_2 \otimes \begin{pmatrix} 1 & 0 \\ 0 & 1 \end{pmatrix}$, $\Gamma_i = \mathrm{I}_2 \otimes (-a_i\ -b_i)$, $\Pi_j = \mathrm{I}_2 \otimes \begin{pmatrix} 1 & 0 \end{pmatrix}$, $\Gamma_j = \mathrm{I}_2 \otimes \begin{pmatrix} 0 & 1 \end{pmatrix}$, $\Pi_{Fi} = \mathrm{I}_2 \otimes \begin{pmatrix} 1 & 0 \\ 0 & 1 \end{pmatrix}$, $\Gamma_{Fi} = \mathrm{I}_2 \otimes (-1 - a_i\ -b_i)$, $\Pi_{Fj} = \mathrm{I}_2 \otimes \begin{pmatrix} 1 & 0 \end{pmatrix}$, and $\Gamma_{Fj} = \mathrm{I}_2 \otimes \begin{pmatrix} 0 & 1 \end{pmatrix}$.

Choose $k_1 = 24$, $k_2 = 5$, $k_3 = 6$, $p = 7/9$, $q = 907/700$, and $M_i = \mathrm{I}_2$, $i = 1, \ldots, 10$, for the observer in (7) and controller in (24). Let initial condition $x_i(0)$ be randomly generated from the interval $[-4, 4]$ and $v_i(0) = \mathbf{0}_4$, $i = 1, \ldots, 10$. The initial states of the leaders are $x_{01}(0) = (0, -0.8, 0, 0.8)^\top$, $x_{02}(0) = (1, 0.8, -1, -0.8)^\top$, and $x_{03}(0) = (1, 0.9, 0, 0.9)^\top$.

The simulation results are shown in Figs. 2–4. Figure 2 shows the motion of the HMAS, where subgroups 1–3 are

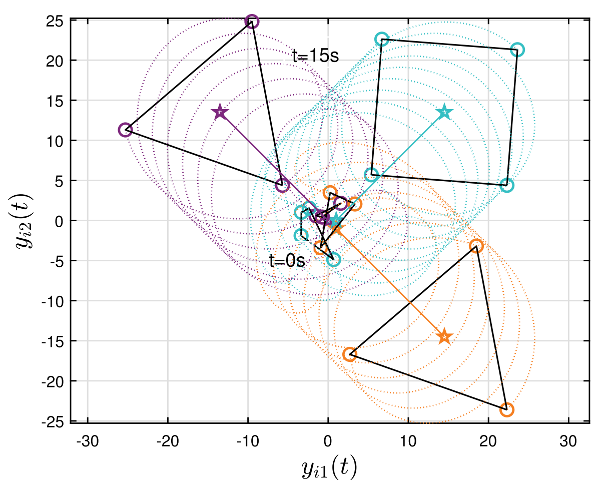

Fig. 2. Motion of the HMAS.

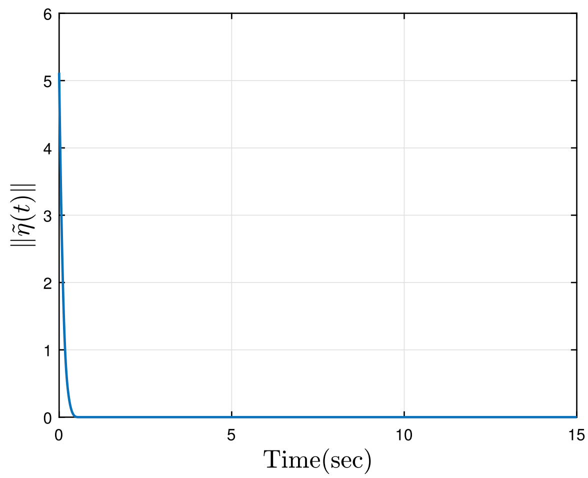

Fig. 3. The distributed observer error.

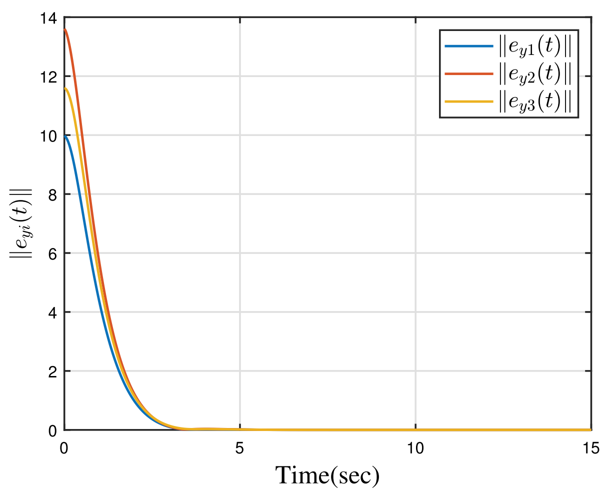

(a)

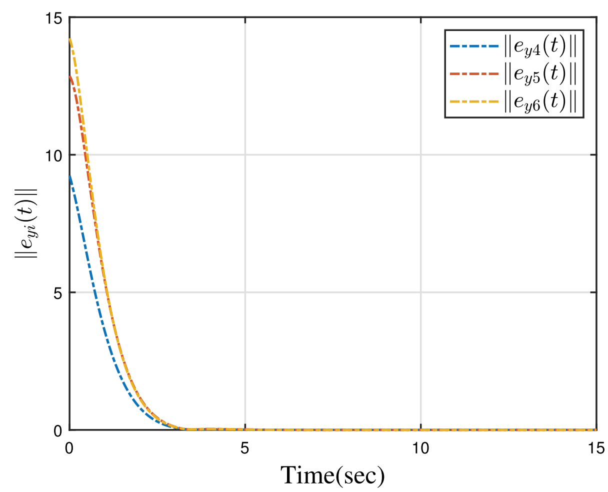

(b)

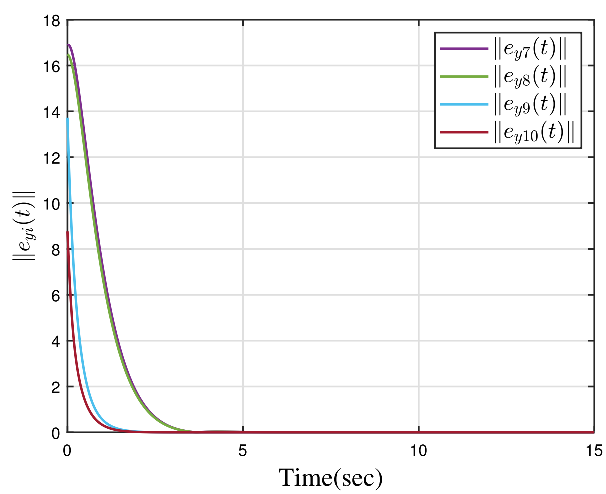

(c)

Fig. 4. The GFT errors with the fixed-time control protocol. (a) Subgroup 1. (b) Subgroup 2. (c) Subgroup 3.

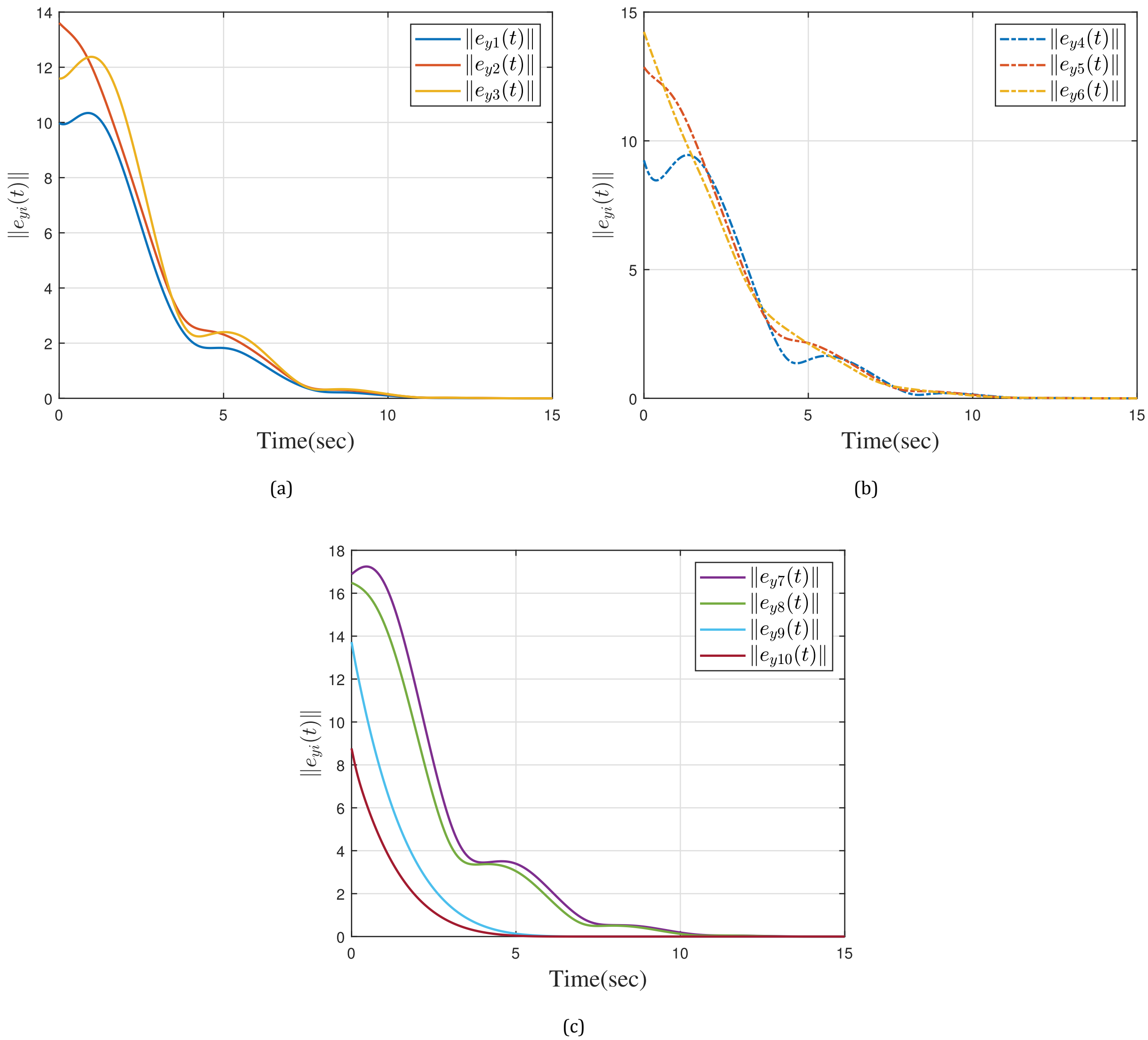

Fig. 5. The GFT errors with the finite-time control protocol. (a) Subgroup 1. (b) Subgroup 2. (c) Subgroup 3.

represented in purple, orange, and cyan, respectively. The leaders are marked with pentagrams, while the followers are denoted by circles. It can be observed from Fig. 2 that the followers in each subgroup form the desired TVF and track their leader in a fixed time. The distributed observer error and the GFT errors are depicted in Figs. 3 and 4, respectively.

For comparison, Fig. 5 depicts the GFT errors for a finite-time control protocol obtained by removing the power index greater than one from our method. The initial conditions for both the HMAS and the distributed observers are set to be identical in this comparison. It is evident from Figs. 4 and 5 that the FXGFT control protocol demonstrates much better performance than the finite-time one.

5. Conclusion

This paper has investigated the FXGFT problem for HMASs under a directed interaction graph. We have proposed a novel distributed FXGFT control protocol comprising a fixed-time observer and a distributed FXGFT controller. It has been shown that, for each subgroup, the followers achieve the desired sub-formation while tracking their subgroup leader. More specifically, the proposed control protocol ensures that the GFT errors converge to zero in a fixed time, and the upper bound of the convergence time does not depend on the initial states. Future research will focus on extending the proposed approach to the sampled-data FXGFT problem for HMASs. Another promising direction is to investigate the robust FXGFT problem for HMASs under external disturbances and other uncertainties.

Acknowledgment

This paper was supported by the Research Grants Council of Hong Kong under Grant Number CityU-11205024.

Appendix A.

Lemma A.1 ([45]). *For any $\zeta_i \in \mathbb{R}$, $i = 1,2,\dots,n$, and any $\iota \in (0,1]$, $(\sum_{i=1}^{n}|\zeta_i|)^{\iota} \le \sum_{i=1}^{n}|\zeta_i|^{\iota} \le n^{1-\iota}(\sum_{i=1}^{n}|\zeta_i|)^{\iota}$. For any $\iota > 1$, $\sum_{i=1}^{n}|\zeta_i|^{\iota} \le (\sum_{i=1}^{n}|\zeta_i|)^{\iota} \le n^{\iota-1}\sum_{i=1}^{n}|\zeta_i|^{\iota}$.*

Lemma A.2 ([33]). *Consider the system $\dot z = g(z,t)$, where $g : \mathbb{R}^n \times [0,\infty) \to \mathbb{R}^n$ is a continuous vector function and $g(0,t) = 0$. Assume there exists a continuous, positive definite function $W(z) : \mathbb{R}^n \to \mathbb{R}$ such that $\dot W(z) \le -a_0(W(z))^{\alpha} - b_0(W(z))^{\beta}$ for all $z \in \mathbb{R}^n$, where $a_0 > 0$, $b_0 > 0$, $0 < \alpha < 1$, and $\beta > 1$. Then, the system is fixed-time stable, with an upper bound on the convergence time given by $T \le \frac{1}{a_0(1-\alpha)} + \frac{1}{b_0(\beta-1)}$.*

Lemma A.3 ([46]). *For a linear system,*

$$\dot x = Ax + Bu, \tag{A.1}$$

where $x \in \mathbb{R}^n$, $u \in \mathbb{R}^m$, A and B are the constant matrices.

Suppose that (A,B) is controllable and the rank$(B) = m$, one can find a nonsingular transformation matrix $T \in \mathbb{R}^{n\times n}$ such that $\xi = Tx = [\xi_1^{\top},\dots,\xi_m^{\top}]^{\top}$. Let ρ_i, $i = 1,\dots,m$, be the controllability index of ξ_i. Then, ξ can be described by $\xi = [\xi_{1,1},\dots,\xi_{1,\rho_1},\dots,\xi_{m,1},\dots,\xi_{m,\rho_m}]^{\top}$ and the dynamics of ξ_i, $i = 1,\dots,m$, have the following form:

$$\begin{cases}\dot\xi_{i,1} = \xi_{i,2},\\ \dot\xi_{i,2} = \xi_{i,3},\\ \vdots\\ \dot\xi_{i,\rho_i} = t_i^{\top}A^{\rho_i}\xi + t_i^{\top}A^{\rho_i-1}Bu,\end{cases}$$

where $t_i^{\top} = i_{r_i}^{\top}T$, $i_k \in \mathbb{R}^n$ is the kth canonical basis vector, and $r_i = \sum_{k=0}^{i-1}(1+\rho_k)$ with $\rho_0 = 0$.

Moreover, define $\xi^{\rho} = [\xi_{1,\rho_1},\dots,\xi_{m,\rho_m}]^{\top} \in \mathbb{R}^m$, one has

$$\dot\xi^{\rho} = G\xi + Mu, \tag{A.2}$$

where

$$G = \begin{pmatrix} t_1^{\top}A^{\rho_1}\\ \vdots\\ t_m^{\top}A^{\rho_m}\end{pmatrix}, \quad M = \begin{pmatrix} t_1^{\top}A^{\rho_1-1}B\\ \vdots\\ t_m^{\top}A^{\rho_m-1}B\end{pmatrix}$$

with M being invertible.

Lemma A.4 ([47]). *Consider a system that is modeled as an nth-order integrator:*

$$\begin{cases}\dot x_1 = x_2,\\ \dot x_2 = x_3,\\ \vdots\\ \dot x_n = u,\end{cases} \tag{A.3}$$

where $x = [x_1,\dots,x_n]^{\top}$ and u are the state and control inputs, respectively.

The fixed-time controller is given as

$$u = -\sum_{j=1}^{n}(\ell_j\,\mathrm{sign}^{\alpha_j}(x_j) + \bar\ell_j\,\mathrm{sign}^{\beta_j}(x_j)), \tag{A.4}$$

where $\ell_j > 0$ and $\bar\ell_j > 0$, $j = 1,\dots,n$, are the constants such that the polynomials $s^n + \ell_n s^{n-1} + \cdots + \ell_2 s + \ell_1$ and $s^n + \bar\ell_n s^{n-1} + \cdots + \bar\ell_2 s + \bar\ell_1$ are Hurwitz. The values $\alpha_1,\dots,\alpha_n$ and $\beta_1,\dots,\beta_n$ can be chosen as $\alpha_{j-1} = \frac{\alpha_j\alpha_{j+1}}{2\alpha_{j+1}-\alpha_j}$ and $\beta_{j-1} = \frac{\beta_j\beta_{j+1}}{2\beta_{j+1}-\beta_j}$, where $j = 2,\dots,n$, $\alpha_{n+1} = \beta_{n+1} = 1$, $\alpha_n = \alpha \in (1-\epsilon,1)$, and $\beta_n = \beta \in (1,1+\bar\epsilon)$ for sufficiently small $\epsilon, \bar\epsilon > 0$.

Moreover, the convergence time satisfies

$$T_c \le \frac{p\lambda_{\max}(P_1)}{(1-p)\lambda_{\min}(Q_1)}\lambda_{\max}^{\frac{1-p}{p}}(P_1) + \frac{q\lambda_{\max}(P_2)}{(q-1)\lambda_{\min}(Q_2)}\lambda_{\max}^{\frac{q-1}{q}}(P_2), \tag{A.5}$$

where $P_i = P_i^{\top} > 0$, $i = 1,2$, satisfy the Lyapunov equation $P_iH_i + H_i^{\top}P_i = -Q_i$, with Q_i being an arbitrary positive definite matrix. The matrices D_i, $i = 1,2$, have the following forms:

$$H_1 = \begin{pmatrix} 0 & 1 & \cdots & 0\\ \vdots & \vdots & \ddots & \vdots\\ 0 & 0 & \cdots & 1\\ -\ell_1 & -\ell_2 & \cdots & -\ell_n\end{pmatrix},$$

$$H_2 = \begin{pmatrix} 0 & 1 & \cdots & 0\\ \vdots & \vdots & \ddots & \vdots\\ 0 & 0 & \cdots & 1\\ -\bar\ell_1 & -\bar\ell_2 & \cdots & -\bar\ell_n\end{pmatrix}.$$

ORCID

Shiyu Zhou
https://orcid.org/0000-0003-3742-4264

Dong Sun
https://orcid.org/0000-0003-3945-4037

Gang Feng
https://orcid.org/0000-0001-8508-8416

References

[1] R. Olfati-Saber and R. M. Murray, Consensus problems in networks of agents with switching topology and time-delays, *IEEE Trans. Autom. Control* **49**(9) (2004) 1520–1533.

[2] J. A. Fax and R. M. Murray, Information flow and cooperative control of vehicle formations, *IEEE Trans. Autom. Control* **49**(9) (2004) 1465–1476.

[3] A. Allam, A. Nemra and M. Tadjine, Cooperative guidance of a multi-quadrotors system with switching and reduced network information exchange: Application to uncooperative target entrapping, *Unmanned Syst.* **12**(04) (2024) 799–818.

[4] Z. Ying and F. Gang, Data-driven leader-following output consensus of discrete-time MASs under DoS attacks, *Unmanned Syst.* **13**(05) (2025) 1307–1318.

[5] Z. Qin, T. Liu, T. Liu, Z.-P. Jiang and T. Chai, Distributed feedback optimization of nonlinear uncertain systems subject to inequality constraints, *IEEE Trans. Autom. Control* **69**(6) (2024) 3989–3996.

[6] F. M. Zegers, P. Deptula, H.-Y. Chen, A. Isaly and W. E. Dixon, A switched systems approach to multiagent system consensus: A relay–explorer perspective, *IEEE Trans. Robot.* **39**(1) (2023) 605–624.

[7] B. Lian, N. T. Nguyen and F. L. Lewis, Distributed cluster containment control of swarms via differential game-theoretic learning, *Unmanned Syst.* **13**(05) (2025) 1283–1294.

[8] Q. Liu, K. Huang, H. Liu, R. Wang and G. Cheng, Multi-domain collaborative task allocation and conflict resolution in unmanned systems under complex constraints, *Unmanned Syst.* **13**(02) (2025) 579–589.

[9] W. Ren, Consensus strategies for cooperative control of vehicle formations, *IET Control Theory Appl.* **1**(2) (2007) 505–512.

[10] W. Xiao, J. Yu, R. Wang, X. Dong, Q. Li and Z. Ren, Time-varying formation control for time-delayed multi-agent systems with general linear dynamics and switching topologies, *Unmanned Syst.* **7**(01) (2019) 3–13.

[11] W. Zhao, H. Liu, F. L. Lewis and X. Wang, Data-driven optimal formation control for quadrotor team with unknown dynamics, *IEEE Trans. Cybern.* **52**(8) (2021) 7889–7898.

[12] X. Dong, Q. Li, Q. Zhao and Z. Ren, Time-varying group formation analysis and design for general linear multi-agent systems with directed topologies, *Int. J. Robust Nonlinear Control* **27**(9) (2017) 1640–1652.

[13] H. Mazeh, H. D. Taghirad and J. Sahili, Distributed consensus formation tracking controller for multi-UAVs: A robust finite-time observer-based approach, *Unmanned Syst.* (2025) 1–19, doi:10.1142/S2301385027500051.

[14] Z. Feng, G. Hu, X. Dong and J. Lü, Discrete-time adaptive distributed output observer for time-varying formation tracking of heterogeneous multi-agent systems, *Automatica* **160** (2024) 111400.

[15] Y. Hua, X. Dong, G. Hu, Q. Li and Z. Ren, Distributed time-varying output formation tracking for heterogeneous linear multi-agent systems with a nonautonomous leader of unknown input, *IEEE Trans. Autom. Control* **64**(10) (2019) 4292–4299.

[16] P. K. Ranjan, A. Sinha, Y. Cao, D. Casbeer and I. Weintraub, Relational maneuvering of leader-follower unmanned aerial vehicles for flexible formation, *IEEE Trans. Cybern.* **54**(10) (2024) 5598–5609.

[17] Z. Shi, Q. Wang, X. Lü, X. Dong, J. Lü and D. Wang, Robust output formation tracking for heterogeneous multiagent systems with multiple leaders: Theory and application, *IEEE Trans. Ind. Electron.* (2025), doi:10.1109/TIE.2025.3589420.

[18] J. Qin and C. Yu, Cluster consensus control of generic linear multi-agent systems under directed topology with acyclic partition, *Automatica* **49**(9) (2013) 2898–2905.

[19] J. Qin, C. Yu and B. D. Anderson, On leaderless and leader-following consensus for interacting clusters of second-order multi-agent systems, *Automatica* **74** (2016) 214–221.

[20] S. Luo and D. Ye, Cluster consensus control of linear multiagent systems under directed topology with general partition, *IEEE Trans. Autom. Control* **67**(4) (2021) 1929–1936.

[21] M. Rehan, A. Basit, I. Ahmed, C. K. Ahn and M. Chadli, Variable threshold-oriented event-triggered cluster consensus for groups of multiagent systems, *IEEE Trans. Cybern.* (2025) doi:10.1109/TCYB.2025.3607967.

[22] J. Hu, P. Bhowmick and A. Lanzon, Distributed adaptive time-varying group formation tracking for multiagent systems with multiple leaders on directed graphs, *IEEE Trans. Control Netw. Syst.* **7**(1) (2019) 140–150.

[23] Y. Lu, X. Dong, Q. Li, J. Lü and Z. Ren, Time-varying group formation-containment tracking control for general linear multiagent systems with unknown inputs, *IEEE Trans. Cybern.* **52**(10) (2021) 11055–11067.

[24] J. Qin, Q. Ma, H. Gao, Y. Shi and Y. Kang, On group synchronization for interacting clusters of heterogeneous systems, *IEEE Trans. Cybern.* **47**(12) (2016) 4122–4133.

[25] S. Zhou and D. Sun, Group formation tracking for heterogeneous linear multi-agent systems under switching topologies, *J. Autom. Intell.* **4**(2) (2025) 108–114, doi:10.1016/j.jai.2025.03.003.

[26] Y. Wang, Z. Wang, H. Zhang and H. Yan, Group formation tracking of heterogeneous multi-agent systems using reinforcement learning, *IEEE Trans. Control Netw. Syst.* **12**(1) (2025) 497–509.

[27] F. Xiao, L. Wang, J. Chen and Y. Gao, Finite-time formation control for multi-agent systems, *Automatica* **45**(11) (2009) 2605–2611.

[28] W. Cao, D. Zhang and G. Feng, Resilient semi-global finite-time cooperative output regulation of heterogeneous linear multi-agent systems subject to denial-of-service attacks, *Automatica* **173** (2025) 112099.

[29] R. Nie, W. Du, Z. Li and S. He, Finite-time consensus control for mass under hidden markov model mechanism, *IEEE Trans. Autom. Control* **69**(7) (2024) 4726–4733.

[30] Y. Salmanpour, M. M. Arefi and J. Cao, Event-triggered adaptive preassigned finite-time consensus control for multiagent systems with nonlinear faults, *IEEE Trans. Cybern.* **54**(12) (2024) 7392–7403.

[31] Z. Li, Y. Wang, Y. Ma, X. Xie and D. Yue, Finite-time event-triggered adaptive fault-tolerant tracking for semi-bounded non-affine systems, *IEEE Trans. Circuits Syst. I, Reg. Papers* **71**(12) (2024) 6094–6104.

[32] D. Zhang, H. Chen, Q. Lu, C. Deng and G. Feng, Finite-time cooperative output regulation of heterogeneous nonlinear multi-agent systems under switching dos attacks, *Automatica* **173** (2025) 112062.

[33] A. Polyakov, Nonlinear feedback design for fixed-time stabilization of linear control systems, *IEEE Trans. Autom. Control* **57**(8) (2011) 2106–2110.

[34] Y. Dong and Z. Chen, Fixed-time synchronization of networked uncertain Euler–Lagrange systems, *Automatica* **146** (2022) 110571.

[35] S. Zhou, D. Sun and G. Feng, Fixed-time formation tracking for heterogeneous linear multi-agent systems with a nonautonomous leader, *IEEE Trans. Control Netw. Syst.* **12** (2025) 1733–1743.

[36] X. Zhuang, J. Liu, H. Li, Y. Wang and J. Luo, A novel fixed time formation for unmanned ground vehicles under communication denial conditions: Relative information control method, *Unmanned Syst.* (2025) doi:10.1142/S2301385026500184.

[37] S. Zhou, D. Sun and G. Feng, Distributed adaptive fixed-time formation tracking for heterogeneous multi-agent systems, *Automatica* **183** (2026) 112632.

[38] W. Cheng, K. Zhang and B. Jiang, Distributed adaptive fixed-time fault-tolerant formation control for heterogeneous multiagent systems with a leader of unknown input, *IEEE Trans. Cybern.* **53**(11) (2023) 7285–7294.

[39] D. Jiang, G. Wen, Z. Peng, J.-L. Wang and T. Huang, Fully distributed pull-based event-triggered bipartite fixed-time output control of heterogeneous systems with an active leader, *IEEE Trans. Cybern.* **53**(5) (2023) 3089–3100.

[40] Y. Shang, Fixed-time group consensus for multi-agent systems with non-linear dynamics and uncertainties, *IET Control Theory Appl.* **12**(3) (2018) 395–404.
[41] L. Hao, X. Zhan, J. Wu, T. Han and H. Yan, Fixed-time group consensus of nonlinear multi-agent systems via pinning control, *Int. J. Control Autom. Syst.* **19**(1) (2021) 200–208.
[42] Y. Zhang, H. Wu and J. Cao, Group consensus in finite time for fractional multiagent systems with discontinuous inherent dynamics subject to Hölder growth, *IEEE Trans. Cybern.* **52**(6) (2020) 4161–4172.
[43] J. Huang, *Nonlinear Output Regulation: Theory and Applications* (Society for Industrial and Applied Mathematics, 2004).
[44] B. Tian, H. Lu, Z. Zuo and H. Wang, Fixed-time stabilization of high-order integrator systems with mismatched disturbances, *Nonlinear Dyn.* **94**(4) (2018) 2889–2899.
[45] G. H. Hardy, J. E. Littlewood and G. Pólya, *Inequalities* (Cambridge University Press, 1952).
[46] D. Luenberger, Canonical forms for linear multivariable systems, *IEEE Trans. Autom. Control* **12**(3) (1967) 290–293.
[47] M. Basin, Y. Shtessel and F. Aldukali, Continuous finite-and fixed-time high-order regulators, *J. Franklin Inst.* **353**(18) (2016) 5001–5012.

Shiyu Zhou received her B.Eng. degree in automation from Northwestern Polytechnical University, Xi'an, China, in 2019, and M.Eng. degree in control science and engineering from the Beihang University, Beijing, China, in 2022. She is currently pursuing Ph.D. degree with the Department of Mechanical Engineering, City University of Hong Kong, Hong Kong. Her current research interests include cooperative control of multiagent systems and synchronization of complex networks.

Dong Sun received his B.Eng. and M.Eng. degrees in precision instrument and mechanology from Tsinghua University, Beijing, China, in 1990 and 1994, respectively, and Ph.D. degree in robotics and automation from The Chinese University of Hong Kong, Hong Kong, in 1997. He is a Chair Professor with the Department of Biomedical Engineering, City University of Hong Kong, Hong Kong, SAR, China.

Professor Sun is currently Fellow of the Canadian Academy of Engineering in Canada, Member of the European Academy of Sciences and Arts, Fellow of the International Academy of Medical and Biological Engineering, Fellow of the American Society of Mechanical Engineers.

Gang Feng received his Ph.D. degree in Electrical Engineering from the University of Melbourne, Australia. He has been with City University of Hong Kong since 2000 after serving as lecturer/senior lecturer at School of Electrical Engineering, University of New South Wales, Australia, 1992–1999. He is now Chair Professor of Mechatronic Engineering. He has been awarded the IEEE Computational Intelligence Society Fuzzy Systems Pioneer Award, the IEEE Transactions on Fuzzy Systems Outstanding Paper Award, Alexander von Humboldt Fellowship, and City University of Hong Kong Outstanding Research Award. He is listed as a SCI highly cited researcher by Clarivate Analytics since 2016. His current research interests include multi-agent systems and control, intelligent systems and control, and networked systems and control.

Professor Feng is IEEE Fellow, and has been Associate Editor of IEEE Transactions on Automatic Control, IEEE Transactions on Fuzzy Systems, IEEE Transactions on Systems, Man & Cybernetics, Part C, Mechatronics, Journal of Systems Science and Complexity, Autonomous Intelligent Systems, Guidance, Navigation & Control and Journal of Control Theory and Applications. He is on the Advisory Board of Unmanned Systems.